A GIS Analysis of Temperature in the Australian Crust

Prame Chopra and Fiona Holgate

Department of Earth & Marine Sciences, Australian National University, ACT 0200, Australia

prame.chopra@anu.edu.au, fiona@ems.anu.edu.au

Keywords: crustal temperature maps GIS

ABSTRACT

Research over the last 10 years has indicated that Australia has a significant geothermal energy resource. Regions of high crustal temperature at depths ≤5km may be economic targets for hot dry rock technology. A new database of temperature measurements made in 5722 wells across Australia has been used to construct improved maps of the spatial distribution of temperature in the Australian crust. The new database, Austherm04, builds upon the earlier work of Somerville et al. (1994) by greatly improving data quality control and by including temperature data from a further 1430 wells. Whilst there has been some enhancement of the overall spatial coverage when compared with the earlier work, the bulk of the new data are still largely clustered within the same provinces that dominate the Somerville *et. al.* dataset. As a result, data distribution across the continent still tends to be rather patchy and irregular with some regions well represented and others not.

An Arc/Info GIS coverage has been built from the Austherm04 database. This coverage was intersected with GIS grids (constructed from Australian mean surface temperature data provided by the Australian Bureau of Meteorology and depth to basement estimates provided by Geoscience Australia) to interpolate the mean surface temperature and depth-to-basement for each well location. Calculations of the crustal temperature at a depth of 5 kilometres at each well location were then made using measured or estimated thermal gradients, the surface temperature estimates and the depth to basement information. In the absence of specific data, a uniform gradient of 25°C/km was assumed for basement rocks. The calculated crustal temperatures at 5 km depth were used to interpolate grids of cell size equal to 0.02 degrees. Interpolation was performed across the continental dataset using geostatistical 'kriging. A variety of semivariogram error-modelling approaches have been tested. To date best results have been obtained with an exponential model.

The crustal temperature maps produced in this study reveal large spatial variations in temperature across continental Australia. Lowest temperatures occur where basement is exposed at the surface such as in the Yilgarn Block, Gawler Craton and Lachlan Fold Belt. High temperatures are associated with thick sedimentary basin cover and the inferred presence of high heat production granites under the sedimentary sequences. Particular examples include the Cooper-Eromanga, Macarthur and Canning Basin regions. Other smaller areas of relatively elevated crustal temperature that may represent future hot dry rock targets include parts of the Sydney, Perth and Murray Basins. Whilst representing significant improvements over the previous Somerville et al. map, the new crustal temperature maps continue to be influenced by artefacts caused by the
strongly heterogeneous spatial distribution of the subsurface temperature data across continental Australia. More sophisticated geostatistical methods and analysis on a province by province basis may offer some improvements but further temperature exploration data will probably be required to significantly improve the resource analysis.

1. INTRODUCTION

The modern Australian continent is located well within the Indo-Australian Plate and is relatively distant from regions of intense tectonic activity. No volcanoes, geysers or other obvious manifestations of significant geothermal energy are apparent at the surface. The most recent volcanism to occur was in south-east South Australia and western Victoria where eruptive events occurred as recently as ~4.5ka (Sheard, 1978, 1983, 1995).

At present Australia makes limited use of low enthalpy geothermal energy at Birdsville, Queensland (electric power generation) and Portland, Victoria (district heating) as well as some use of warm geothermal waters for spas (Chopra, this volume). Notwithstanding the modest utilization of geothermal energy in Australia, Somerville et al. (1994) showed that significant geothermal resources do in fact exist. In that study a database was assembled from all the subsurface temperature measurements available at the time. Temperature data from a total of 4292 boreholes were compiled in the Geotherm93 database (Figure 1). As shown in the figure, the spatial distribution of this data is very heterogeneous. Much of the data is sourced from petroleum exploration and production wells and as a result there is a strong tendency for it to cluster within known hydrocarbon provinces.
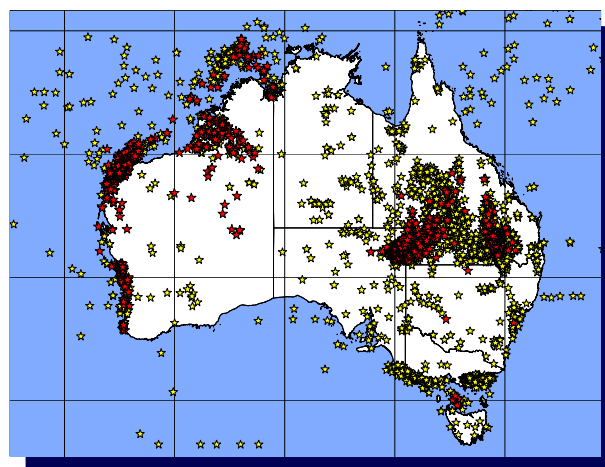

Figure 1 Locations of temperature data in the Geotherm03 database of Somerville et al. (1994) (yellow stars) and Austherm04 from this study (red stars).

The Geotherm93 database was used by Somerville et al. (1994) to estimate crustal temperatures at a common depth across the continent, rather than as a basis for a more

customary heat flow study (e.g. Cull, 1982). This approach was necessary because rock samples were not collected by the companies that drilled the wells. As a consequence there are no measurements of rock thermal conductivities available for the calculation of heat flow.

Somerville et al. chose a depth of 5 km as a practical limit for the economic extraction of geothermal energy, given the rapid increase in the cost of drilling with depth. They extrapolated each temperature recorded in the database from its individual depth of measurement down to 5 km using a mix of manual and geographic information system (GIS) methods. Manual estimates of the Mean Annual Surface Temperature (MAST) at each well location were read from a 1° square geographic grid extended across the continent. This grid was derived graphically from a set of MAST point estimates provided by the Australian Bureau of Meteorology. In a second manual process, Somerville et al. (1994) estimated the mean depth to basement on another 1° geographic grid. For each 1° cell an estimate of the average depth to basement (i.e. the mean sediment thickness) was made by visual inspection of available data.

By combining the borehole temperature and depth measurements in the database with their manual results, Somerville et al. (1994) were able to derive temperature estimates for the sedimentary basin/basement interface. These estimates were then extended to 5 km depth by assuming, in the absence of specific data, that the geothermal gradient in basement rocks is a uniform 25°C/km. The interpolated temperature surface represented in the Somerville et al. (1994) map shown in Figure 2 was derived in a GIS using Delaunay Triangulation to develop an irregular triangulated network (TIN). The TIN procedure coped with the strongly heterogeneous data distribution of Geotherm93 but had the disadvantage of producing pronounced triangular anomalies. Such features are geologically unrealistic both in shape and in the sharp step-like character visible in parts of the interpolated temperature surface (Figure 2).

The present study updates the Somerville et al. (1994) work by incorporating sub-surface temperature data acquired since 1993. Improved quality control has been applied to all data to filter out erroneous and inconsistent results. More rigorous GIS methods have been introduced to estimate MAST and depth to basement, and both these parameters have been interpolated on a finer 0.2° geographic grid. Lastly, an alternative geostatistical method, kriging, has been used to interpolate the temperature surface at 5km depth. By using kriging, the triangular anomalies prevalent in the Somerville et al. (1994) results are avoided.

2. THE AUSTHEM04 DATABASE

The Austherm04 database has been built from the earlier Geotherm93 database of Somerville et al. (1994). The existing 4292 records in Geotherm93 for which temperature data were available were assessed for data quality and for consistency with surrounding results. Data from an additional 1430 sub-surface temperature measurements were added to the database representing wells drilled in the period 1993 to early 2004. In the case of 90 Cooper Basin wells, the temperature data in the database were cross-checked against information included in open-file field logs.

The additional data added to Austherm04 have slightly improved the spatial coverage of the database (see Figure 1). However, since the bulk of the new data are again sourced from petroleum exploration and production wells,

most still cluster within the same geographic concentrations that dominate the Geotherm93 coverage.
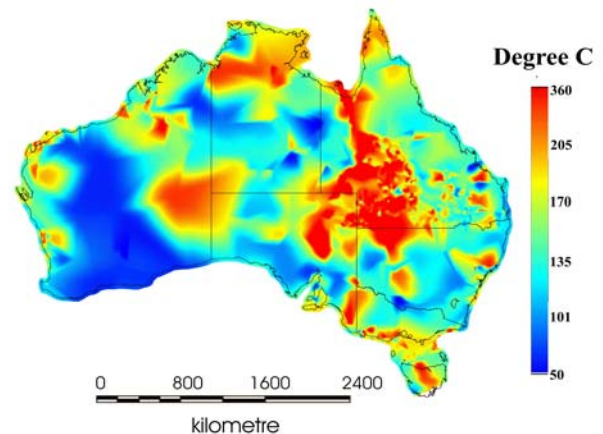

Geotherm93 Estimated Temperature at 5km

Figure 2 Temperature resource map of Somerville et al. (1994) generated from the Geotherm93 database using a mixture of manual and GIS methods.

3. ESTIMATING MEAN ANNUAL SURFACE TEMPERATURE

Estimates of the mean annual surface temperature (MAST), both onshore and offshore, were provided by the Australian Bureau of Metereology. A total of 22 244 point estimates of MAST were provided on a 0.25° grid (see Figure 3a). A GIS grid was constructed from these data using the geostatistical technique known as Ordinary Kriging. This method is based on the estimation of regionalised variables over a finite geographic distribution known as a neighborhood (Burrough and McDonnell, 1998). Points contained within a neighborhood are assumed to be spatially correlated and can be used to interpolate other values within that same space. With increasing distance the degree of spatial correlation declines until it approaches that of the entire population. Thus as the distance between an interpolated point and any point datum increases, the ability of that datum to predict the interpolated value falls. In practice, the degree of spatial correlation can be assessed in terms of the semivariance between a given point location and all the points in the input data set. This can be plotted in a semivariogram which graphs the change in semivariance with increasing distance. The degree of fitness of the kriged interpolation is assessed by comparing the semivariogram results with the results of theoretical models based on different assumed spatial dependencies. Typical models used for this purpose include spherical, circular, exponential, Gaussian and linear dependencies.

A variant of kriging known as Universal Kriging was used to interpolate MAST values in this study. Universal Kriging is suited to interpolation of data sets that incorporate an overall spatial gradient in the parameter being interpolated such as occurs here between surface temperature and latitude. The results shown in Figure 3b clearly depict the temperature discontinuity at the continental margin and the increasing value of MAST with decreasing latitude. The influence of topography on MAST is also clearly seen, particularly in south east of the continent where the areas of higher elevation are associated with lower mean annual surface temperature estimates.
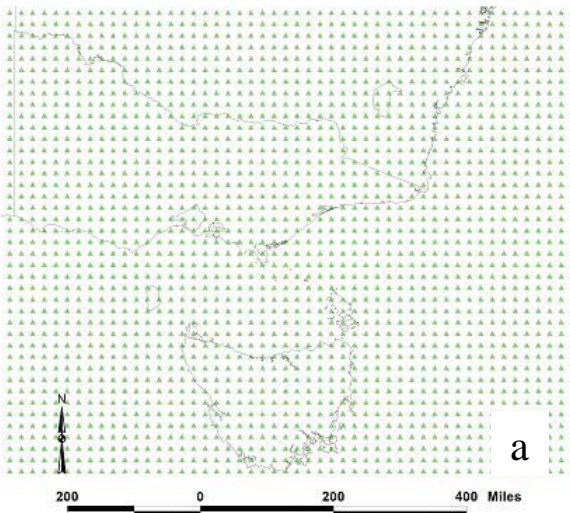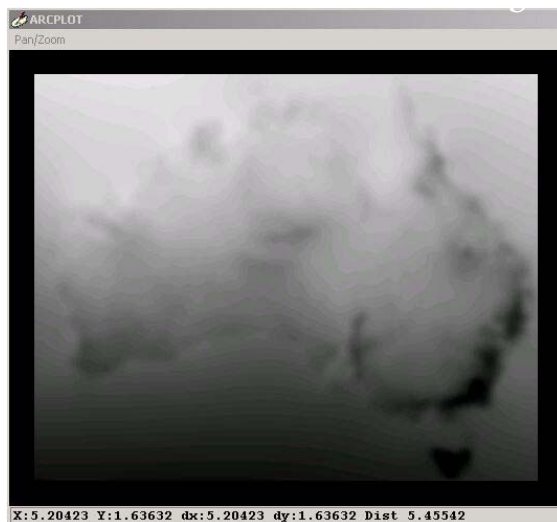
Figure 3 Part of the spatial coverage of the Mean Annual Surface Temperature (MAST) data (Fig. 3a) and the Australia-wide map derived from the whole

MAST dataset using universal kriging (Fig. 3b).

The MAST grid was intersected with the well locations in the GIS to produce an estimate of MAST for each well. These values could then be used together with depth and subsurface temperature data to derive straight-line estimates of the geothermal gradient for each well as is discussed below.

4. ESTIMATING DEPTH TO BASEMENT

The thickness of sedimentary basin cover represented by the "depth to basement" is an important parameter for subsurface temperature estimation. Sedimentary rocks often have relatively low thermal conductivities and may sustain higher than average geothermal gradients. Values approaching 100°C/km are not unusual, particularly when coal-bearing rocks and carbonaceous shales are present. For this reason it is important to quantify the thickness of sediment in locations where borehole temperature measurements have been made.

Line data representing sedimentary isopachs were provided in GIS format by Geoscience Australia (Figure 4a). These data were used to derive a continent-wide grid of depth to basement using the GIS. A minimum curvature spline method was used in this case because kriging was unable to produce geologically realistic results from the isopach line data. The kriging methods all produced large data spikes

and other interpolation noise. The results for the minimum curvature spline method are shown in Figure 4b with regions of greater depth to basement shown in lighter shades. As before, the new GIS grid was intersected with the well locations coverage. In this case, estimates of the depth to basement at each well location were produced
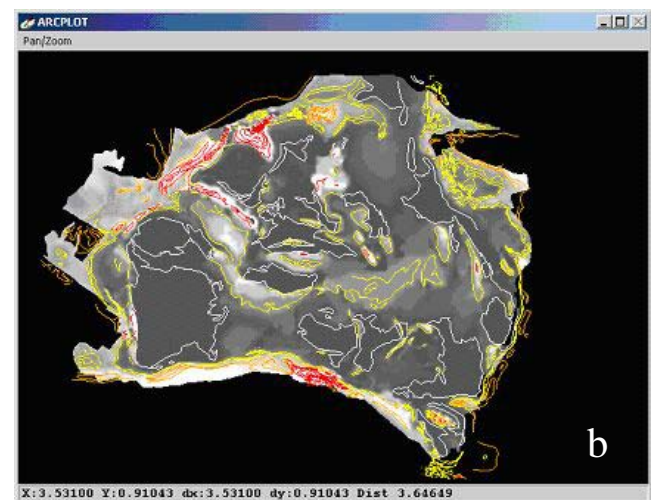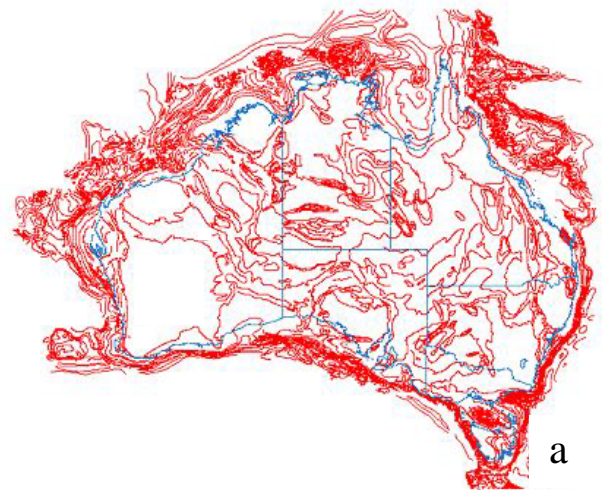

Figure 4 Sedimentary basin isopach data provided by Geoscience Australia (Fig. 4a) and the map of depth to basement derived from these data using a minimum curvature spline technique (Fig. 4b). In Fig. 4b lighter shades represent greater depths and contours represent depths of 0 metre (white), 1999 < depth <3000 metre (yellow), 5000< depth < 8000 metre (orange) and depth > 9000 metre (red).

5. ESTIMATING TEMPERATURE AT 5KM DEPTH

One dimensional extrapolations were used to estimate the temperature at 5km depth at each well location in the Austherm04 database. Six scenarios were developed, each utilizing a uniform geothermal gradient of 25°C/km for basement rocks. The six scenarios are shown in Figure 5.

For example in Scenario 2, the temperature has been measured in a given well at a depth that places it within the sedimentary basin sequence. In this situation, the geothermal gradient is first determined by straight-line interpolation between the Earth's surface and the depth of measurement recorded in Austherm04, using the MAST value previously generated for this well. The calculated gradient is extended to the estimated depth of the sedimentary basin / basement interface. As this interface

3

lies above 5km depth in Scenario 2, the temperature estimated at this depth is then further increased at the rate of 25°C/km (adopted for all basement rocks in this study), to derive a final estimate of the temperature at 5km.
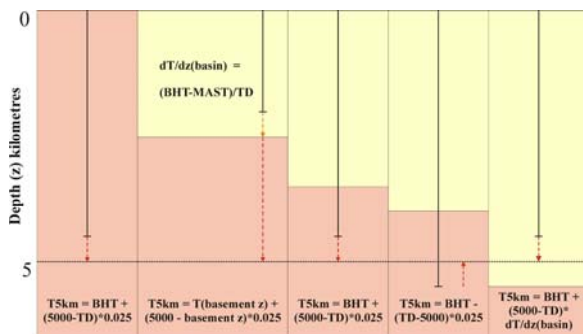

Figure 5 Six scenarios used to estimate the temperature at 5km depth (T5km) from the information in the Austherm04 database. In the figure yellow represents sedimentary basin fill and pink represents basement. BHT = bottom hole temperature, TD = total depth in metre and dT/dz is the geothermal gradient. Scenarios 1-6 are numbered from left to right.
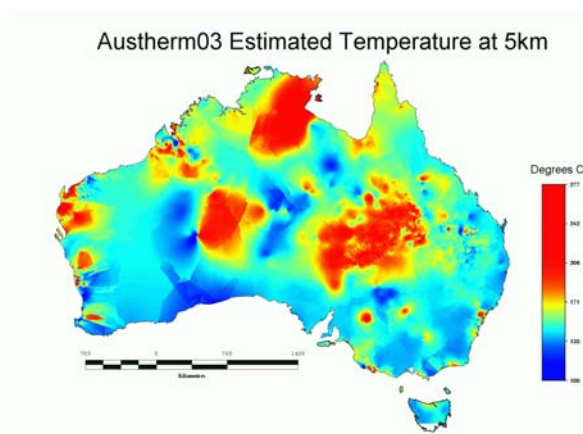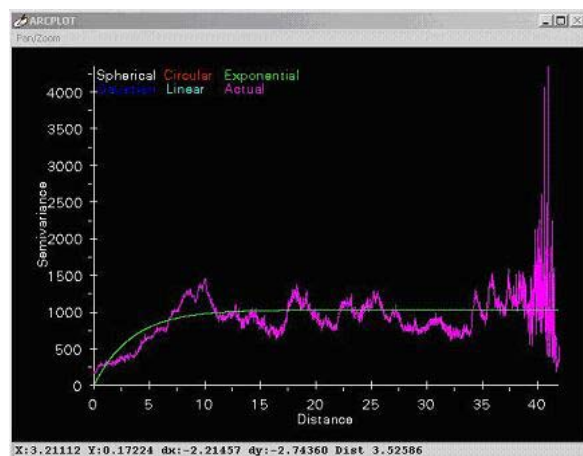

Figure 6 Results obtained from ordinary kriging of the estimates of temperature at 5km. The semivariogram results are shown in Fig. 6a in magenta with an exponential spatial model superimposed in green. The associated kriged map of temperature at 5km is shown in Figure. 6b.

The result of this 1D extrapolation process was a set of estimates of the temperature at 5km depth at 5306 locations across onshore and offshore Australia. These point estimates were then used to spatially interpolate estimates of the temperature at 5km on a regular 0.02° geographic grid using Ordinary Kriging. Several different spatial dependence models were used to evaluate the semivariograms of the kriged results. The best results appeared to be produced using an exponential model. An example semivariogram is shown in Figure 6a and the resulting kriged surface representing the temperature at 5km depth across the continent is shown in Figure 6b.

Some general conclusions may be drawn from the distribution of interpolated temperatures shown in Figure 6. First, the lowest estimated temperatures are associated with regions of outcropping basement such as the Yilgarn Block, Gawler Craton and Lachlan Fold Belt. Whilst this is not surprising, given the age of much of this crust, it is also a likely reflection of the assumption for this work that all basement has a geothermal gradient of 25°C/km. This simplifying assumption was made necessary by the generally very low density of temperature observations available in Austherm04 for basement terranes. A second observation from Figure 6 (when read in conjunction with Figure 4) is that regions of high temperature are often associated with relatively thick sedimentary basin cover. Examples include the Cooper-Eromanga Basin of central Australia, the Macarthur Basin of northern Australia and the Canning Basin region of north-west Western Australia. Other smaller areas of relatively elevated crustal temperature that may represent future hot dry rock targets include parts of the Sydney, Perth and Murray Basins.

6. DISCUSSION

The GIS-derived temperature map shown in Figure 6b is based on more rigorous methods than the earlier map of Somerville et al, 1994 shown in Figure 2. By combining finer grained GIS estimations of mean annual surface temperature and depth to basement with a scenario-based estimator of subsurface temperature, more reliable estimates of point-located temperature at 5km have been derived. As shown in Figure 7, the additional data available in Austherm04, its improved quality control and the use of more sophisticated geostatistical methods to interpolate the temperature results across the continent have produced a better final map.

Interpolation errors are still present in the new image however and the kriging process has clearly been adversely influenced by the strongly heterogeneous distribution of the data in the Austherm04 database. In areas with high densities of temperature observations the kriging process has been well constrained and smooth variations in interpolated temperature and rounded anomalies are typical (e.g. Figure 7b). However in areas where there is little or no data, structures that are clearly spurious are apparent in the kriged results. A prime example is found in the south-eastern region of Western Australia. Austherm04 contains no data for this area (see Figure 1) and as a result the kriging process is poorly constrained. Hence the large linear anomaly boundary structures present in this part of the map in Figure 6b are artifacts. Such artifacts are unlikely to be removed from future temperature maps without the addition of new temperature data in these areas. However, very little of the temperature data in Austherm04 has been collected specifically for geothermal exploration. The majority of the data are sourced from petroleum and, to a lesser extent, mineral exploration with a few data collected from groundwater bores. Since this data provenance is expected to continue, it is unlikely that the current "spatial holes" in the database will be filled in soon.
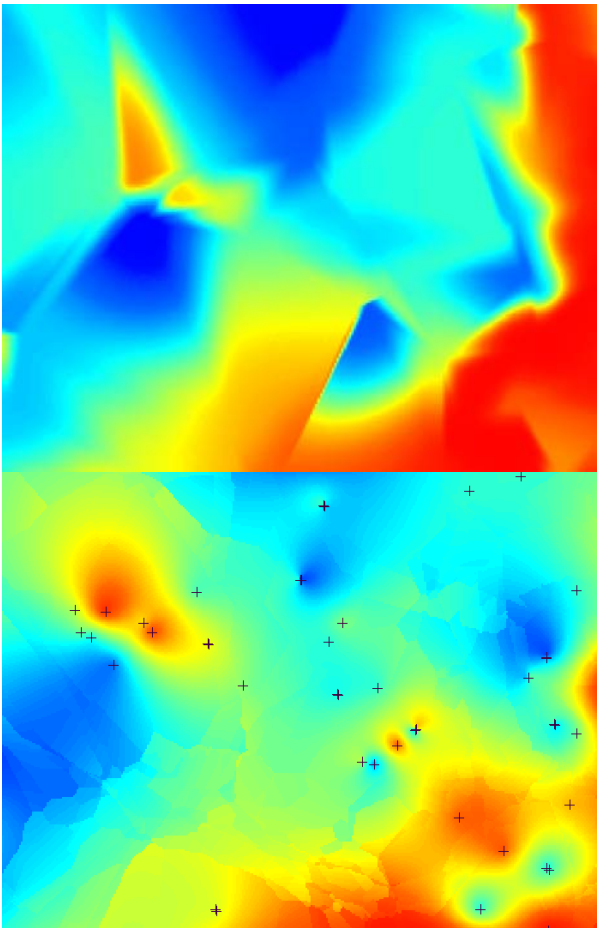
Figure 7 Comparisons of part of the earlier map of Somerville et al, 1994 (top) with the results of this study (bottom). The pronounced triangular anomalies and sharp discontinuities present in the earlier map are less evident in the new results. Interpolation artefacts are nevertheless still present. The area displayed in each case is from central Australia and is bounded by 134.3ºE, 20.6ºS and 141ºE, 25.5ºS.

With this deficiency in mind an approach has been trialled that uses geological information to help confine the errors introduced by the interpolation. Specifically, the Australian Tectonic Elements Map (Shaw et al., 1996) has been used to restrict the region of influence of data in the Austherm04 database to geological blocks of common tectonic provenance. The tectonic elements map divides the basement of the Australian continent into 335 tectonic elements each of which has a similar magnetic and gravity character that is assumed to relate to crustal-scale domains of like composition and/or structural configuration. The tectonic elements data are displayed in Figure 8 with the previous kriging results and the Austherm04 data.

Figure 9 provides a detailed view of part of the Northern Territory from Figure 8. Here a substantial region of northern Australia is inferred to have significantly elevated temperatures at 5km depth. This region has been mapped by kriging the Austherm04 points shown and without considering the tectonic elements map. Interestingly, the thermal domains within this region seem to largely mirror the tectonic element boundaries defined by Shaw et al. (1996). This agreement suggests that tectonic element boundaries may also represent thermal discontinuities in the subsurface
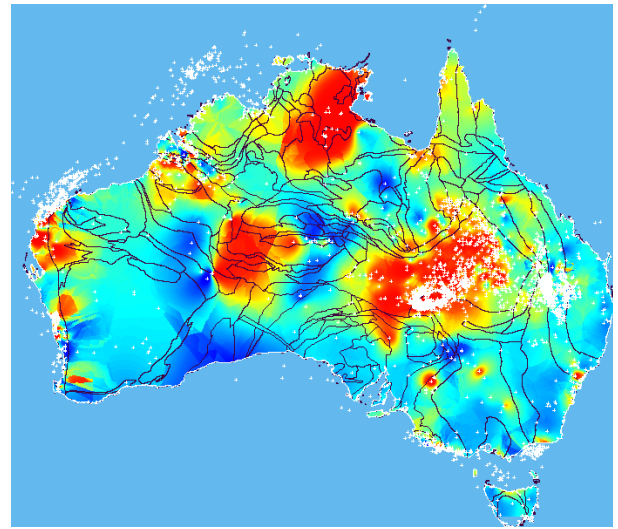

Figure 8 The Australian Tectonic Elements Map (Shaw et al., 1996) combined with the points of the Austherm04 database and the kriging results of Figure 6b.
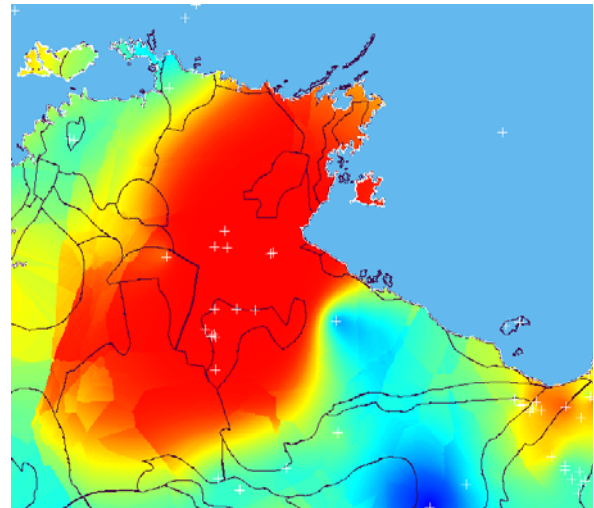

Figure 9 Detail from Figure 8 showing part of the Northern Territory. The Australian Tectonic Elements Map (Shaw et al., 1996) is represented by the black lines and the points of the Austherm04 database are shown as white crosses. The kriging results of Figure 6b are shown underneath the vectors. Note that the outlines of the pronounced thermal anomaly show some broad associations with some of the tectonic element boundaries.

A similar close-up is shown in Figure 10 for the western part of Western Australia. Here the tectonic elements representing the Palaeozoic Perth Basin and an adjoining part of the Archaean Yilgarn Block are shown together with the available Austherm04 data locations. As the Perth Basin is prospective for petroleum, a large number of exploration wells have been drilled and subsurface temperatures measured. Conversely, the Yilgarn Block to the east has no petroleum potential and as a consequence there have been few boreholes drilled in which temperatures have been recorded. The widely different ages and rock types characterising these two tectonic elements are also reflected in significantly different geothermal gradients. The available data in Austherm04 for the Yilgarn Block have calculated geothermal gradients with a mean value of 11°C/km (from 14 wells with an average depth of measurement of 410 metre). On the other hand, the onshore Perth Basin wells shown in Figure 10 have a mean

calculated geothermal gradient of 31°C/km (from 147 wells with a mean depth of temperature measurement of 2450 metre).

Typical artefacts introduced during kriging of regions of sparse data are evident in the kriged image of Figure 10. The lack of data over the Yilgarn Block has resulted in strong linear artefacts extending eastward from Austherm04 wells sited in the Perth Basin. From a geological point of view these structures are highly unlikely.
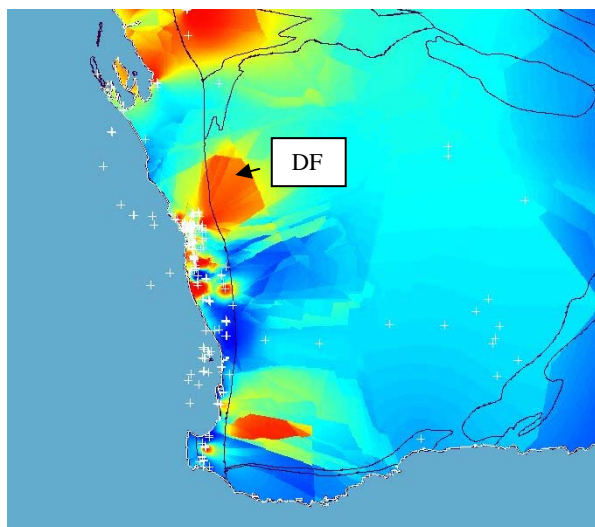

Figure 10 Detail from Figure 8 showing Western Australia between 111.1° and 123.8°E longitude, 24.5° and 35.7°S latitude. The Australian Tectonic Elements Map (Shaw et al., 1996) is represented by the black lines and the points of the Austherm04 database are shown as white crosses. The kriging results of Figure 6b are shown underneath the vectors. The north-south trending tectonic element boundary near the centre of the figure (the Darling Fault, labelled DF) separates the Archaean Yilgarn Block to the east from the Paleozoic Perth Basin to the west. The apparent structures in the temperature data east of the boundary are artefacts generated from the data on the western side of the boundary.

In Figure 11, the influence of the Perth Basin data has been restricted to the confines of the tectonic element in which they fall. Similarly, the temperature at 5km of the juxtaposed region of the Yilgarn Block to the east has been calculated only from the Austherm04 data points that actually fall within its boundaries. The result is a significant discontinuity in the inferred temperature at 5km depth across the tectonic element boundary. At the scale of this map, such a discontinuity is probably geologically plausible, even over long geological time scales, given the widely different geology on either side of the boundary.

Similar analyses are being carried out across Australia on a tectonic element by tectonic element basis where practicable. In some cases there are too few data points available in Austherm04 to sustain such an approach and results have to be aggregated across several elements. In other cases, such as the Cooper-Eromanga element, there are very large numbers of data and inconsistencies due to variable data quality impact on the analysis.
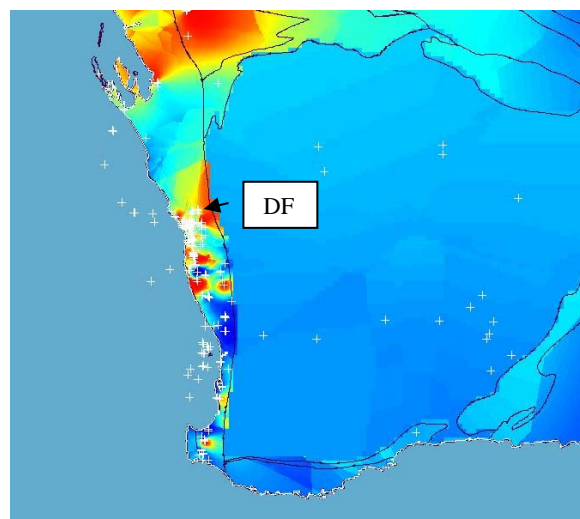

Figure 11 Same area as Fig. 10 showing part of Western Australia. The Australian Tectonic Elements Map (Shaw et al., 1996) is represented by the black lines and the points of the Austherm04 database are shown as white crosses. Kriging results shown underneath the vectors have been calculated separately for the Yilgarn Block and Perth Basin tectonic elements. The cell size of the kriged grid over the Yilgarn Block has been set to 0.1 degrees in view of the sparse input data. The tectonic element boundary (the Darling Fault, labelled DF) now represents a significant temperature discontinuity.

7. CONCLUSIONS

Geographic Information System techniques have been used to generate a map of the estimated temperature at a depth of 5km in the Australian crust from a database of 5722 subsurface temperature measurements. Temperature measurements in the Austherm04 database were first extrapolated in depth to 5km using 6 scenarios and GIS grids representing mean annual surface temperature and sedimentary basin thickness (depth to basement). Interpolation of temperature estimates at 5km depth across the continent used the Ordinary Kriging geostatistical method. Semi-variogram analysis suggested that kriging was best performed with an exponential spatial dependence.

Improvements in the quantity and quality of data in the Austherm04 database over that available to Somerville et al. (1994), combined with more rigorous GIS methods has produced an improved temperature map compared with that of the earlier study. However, the strongly heterogeneous spatial data distribution still produces significant interpolation artifacts in areas of sparse data coverage. Incorporating geological information into the interpolation process can reduce these artifacts in areas where sufficient subsurface temperature data are available.

The crustal temperature maps that have been generated suggest that lowest temperatures at 5km depth occur in areas where basement rocks are exposed at the surface such as in the Yilgarn Block, Gawler Craton and Lachlan Fold Belt. High temperatures are most commonly associated with areas of thick sedimentary basin cover. Examples include the Cooper-Eromanga, Macarthur and Canning Basin regions. Other smaller areas of relatively elevated crustal temperature that may represent future hot dry rock targets include parts of the Sydney, Perth and Murray Basins.

REFERENCES

Burrough, P. A. and McDonnell, R. (1998). *Principles of Geographical Information Systems*. Oxford University Press, Oxford, pp. 333.

Chopra, P.N. (2005). Status of the Geothermal Industry in Australia, 2000-2005, *Proceedings of the World Geothermal Congress, 2005, Antalya, Turkey*, this volume.

Cull, J.P. (1982). An appraisal of Australian heat flow data, BMR Journal of Australasian Geology & Geophysics, 7, 11-21.

Shaw, R.D., Wellman, P., Gunn, P., Whittaker, A.J., Tarlowski, C. & Morse, M., (1996). Guide to using the Australian Crustal Elements Map. Australian Geological Survey Organisation Record 1996/30.

Sheard, M.J. (1978). Geological history of the Mt Gambier Volcanics area, South Aust. Dept. Mines and Energy, Mineral Information Series, 12pp.

Sheard, M.J. (1983). Volcanoes. In: M.J. Tyler, C.R.T. Twidale, J.K. Ling and J.W. Holmes (eds)., *Natural History of the South East*, Royal Society of South Australia, Adelaide, Australia, pp. 7-14.

Sheard, M.J. (1995). In: J.F. Drexel and W.V. Preiss (eds.), *The Geology of South Australia, Volume 2, The Phanerozoic*, Bulletin South Australian Geological Survey, 54, pp264-268.

Somerville, M., Wyborn, D., Chopra, P., Rahman, S., Estrella, D. and T. Van der Meulen (1994). "Hot dry rock feasibility study." Energy Research and Development Corporation, Australia, Report 94/243.